

### Test of time-reversal invariance in <sup>131</sup>Xe

J. L. Gimlett, H. E. Henrikson, and F. Boehm  
 California Institute of Technology, Pasadena, California 91125

J. Lerner  
 Argonne National Laboratory, Argonne, Illinois 60439  
 (Received 3 August 1981)

An experiment has been performed to test the time-reversal symmetry in the emission of the mixed *E*2 and *M*1 364 keV  $\gamma$  transition in <sup>131</sup>Xe. The phase angle  $\eta$  between the multipole transition amplitudes was measured by observing the angular distribution of the linear polarization of the  $\gamma$  ray emitted from a <sup>131</sup>I source polarized at low temperature (30 mK obtained with a dilution refrigerator). A Compton polarimeter was used to measure linear polarization. The <sup>131</sup>Xe transition was selected to minimize atomic final state effects which simulate time-reversal violation. A value  $\sin \eta = (-1.1 \pm 1.1) \times 10^{-3}$  was obtained for the transition, consistent with time-reversal invariance.

RADIOACTIVITY <sup>131</sup>Xe; measured linear polarization of 364 keV  $\gamma$  from polarized nuclei, time-reversal test; deduced relative phase of *E*2, *M*1.

#### I. INTRODUCTION

Aside from the famous case of the neutral kaon decay, no violation of time-reversal (*T*) invariance has been observed. The investigation of the time-reversal symmetry with increasingly higher sensitivity in other areas of physics remains an important experimental challenge.

Among the most sensitive tests of time-reversal invariance in nuclear systems are correlation experiments involving nuclear radiation. Experiments based on the *T*-odd combination of observables

$$(\langle \vec{J} \rangle \cdot \vec{k} \times \vec{E})(\langle \vec{J} \rangle \cdot \vec{k})(\langle \vec{J} \rangle \cdot \vec{E}) \quad (1)$$

have been particularly successful in providing precise limits on *T* violation in nuclear transitions.<sup>1,2</sup> In this expression  $\langle \vec{J} \rangle$  is the expectation value of the spin of a nucleus in an initial excited state and  $\vec{E}$  is the linear polarization vector of a gamma ray with momentum  $\vec{k}$  emitted from that state.

In a nuclear electromagnetic transition of mixed multipolarity, time-reversal noninvariance would manifest itself as a relative phase shift between the transition amplitudes  $A(L\pi)$  and  $A(L'\pi')$  of the two competing multipoles. This phase,  $\eta = \eta(L\pi)$

$-\eta(L'\pi')$ , is related to the "mixing ratio"  $\delta$  by

$$\delta = A(L\pi)/A(L'\pi') = \pm |\delta| e^{i(\eta+\xi)}. \quad (2)$$

Experiments which measure *T*-odd correlations [e.g., Eq. (1)] are sensitive to the imaginary component of  $\delta$ , i.e.,  $\sin(\eta+\xi)$ . Contributing to this component is the "final state" phase shift  $\xi = \xi(L\pi) - \xi(L'\pi')$ . This phase shift arises from the interaction of the radiated photon with the surrounding atomic electrons, and is indistinguishable from the time-reversal phase  $\eta$  in a correlation experiment.<sup>2</sup> In a transition where  $\xi$  is known to be negligible, observation of a nonvanishing value of  $\eta$  would constitute evidence for time-reversal noninvariance.

The parameters  $\xi(L\pi)$  depend on the multipolarity and energy of the nuclear transition, as well as the atomic number *Z*. In general  $\xi$  is largest at low energies and for *Z* ~ 60, and is smallest for high energy, low *Z* transitions. Calculations for  $\xi$  have been published by Goldwire and Hannon,<sup>3</sup> and more recently by Davis *et al.*<sup>4</sup>

We have previously described an experimental technique based on the measurement of the *T*-odd correlation Eq. (1) from the polarization distribution of radiation emitted from nuclei polarized at

low temperature.<sup>1,2</sup> Experiments based on the mixed 129 and 122 keV transitions of <sup>191</sup>Ir and <sup>57</sup>Fe yielded phases  $(\eta + \xi) = (-4.8 \pm 0.2) \times 10^{-3}$  and  $(\eta + \xi) = (-0.3 \pm 0.6) \times 10^{-3}$ , respectively, in substantial agreement with the calculations of Ref. 4 which give  $\xi(^{191}\text{Ir}) = (-4.3 \pm 0.4) \times 10^{-3}$  and  $\xi(^{57}\text{Fe}) = (-0.60 \pm 0.03) \times 10^{-3}$ . Limits for  $\eta$  were obtained by subtracting the calculated  $\xi$  from the measured  $(\eta + \xi)$ . In order to directly measure the time-reversal phase  $\eta$ , however, one must select a transition where  $\xi$  is negligible at the given level of experimental precision. In this paper we summarize the results of a similar time-reversal experiment based on the mixed 364 keV transition of <sup>131</sup>Xe. This transition has a calculated<sup>4</sup> final state phase  $\xi = -1 \times 10^{-4}$ , an order of magnitude smaller than the final state effect for the <sup>191</sup>Ir and <sup>57</sup>Fe cases.

## II. PRINCIPLES OF THE EXPERIMENT

### A. Angular distribution from oriented nuclei

The angular and linear polarization distribution of gamma radiation emitted from an axially symmetric oriented source may be written as a combination of three terms<sup>2</sup>:

$$W(\theta, \phi) = W_1(\theta) + W_2(\theta, \phi) + W_3(\theta, \phi), \quad (3)$$

with  $\theta$  the angle between the radiation emission vector  $\vec{k}$  and the nuclear orientation vector  $\vec{J}$ , and  $\phi$

the angle between the linear polarization vector  $\vec{E}$  and the  $\vec{J} - \vec{k}$  plane.  $W_1$  is the directional (intensity) distribution, and  $W_2$  and  $W_3$  are, respectively, the  $T$ -even and  $T$ -odd linear polarization distribution components. The following equations summarize the expressions of Ref. 2:

$$W_1(\theta) = \sum_{\lambda=\text{even}} Q_\lambda B_\lambda U_\lambda A_\lambda P_\lambda(\cos\theta), \quad (4)$$

$$W_2(\theta, \phi) = \sum_{\lambda=\text{even}} Q_\lambda B_\lambda U_\lambda A_{\lambda 2} 2 \left[ \frac{(\lambda-2)!}{(\lambda+2)!} \right]^{1/2} \times P_\lambda^2(\cos\theta) \cos 2\phi, \quad (5)$$

$$W_3(\theta, \phi) = \sum_{\lambda=\text{odd}} Q_\lambda B_\lambda U_\lambda A'_{\lambda 2} (2i) \left[ \frac{(\lambda-2)!}{(\lambda+2)!} \right]^{1/2} \times P_\lambda^2(\cos\theta) \sin 2\phi. \quad (6)$$

In these equations the  $B_\lambda$  are nuclear orientation coefficients, and depend on the initial nuclear spin  $I$  and the Boltzmann exponent  $(\mu B / IkT)$ ,  $U_\lambda$  and  $A_\lambda$  are deorientation and angular distribution coefficients, respectively,  $P_\lambda$  and  $P_\lambda^2$  are associated Legendre polynomials of order  $\lambda$ , and the  $Q_\lambda$  are detector solid angle corrections. The  $B_\lambda$ ,  $U_\lambda$ , and  $A_{\lambda 2}$  coefficients are tabulated by Krane.<sup>5,6</sup> Expressions for  $A_{\lambda 2}$  and  $A'_{\lambda 2}$  are presented in Ref. 2.

The lowest-order nonzero  $T$ -violating term ( $\lambda=3$ ), corresponding to the vector correlation of Eq. (1), becomes<sup>2</sup>

$$W_3(\theta, \phi) R Q_3 B_3 E_p \left[ |\delta| e^{i\pi} \sin(\eta + \xi) / (1 + |\delta|^2) \right] P_3^2(\cos\theta) \sin 2\phi. \quad (7)$$

The quantity  $R$  is an abbreviation for spin coefficients:

$$R = -(1/\sqrt{30}) U_3 f_3 (LL') F_3 (LL' I_f I_i).$$

Measurement of the term  $W_3$  requires a detection system sensitive to photon linear polarization (with polarization efficiency  $E_p$ ).

$W_3$  arises through the interference of two multipole components of the gamma transition, and is proportional to the phase  $(\eta + \xi)$ . It is a maximum for the angles  $\theta_m = 54.7^\circ \pm n\pi$ ,  $\phi_m = 45^\circ \pm n\pi/2$  [for which  $W_2(\theta, \phi)$  and the  $\lambda=2$  term of  $W_1(\theta, \phi)$  fortuitously vanish]. Noticing that  $W_3$  changes sign under the transformation  $\theta \rightarrow \pi - \theta$ ,  $\phi \rightarrow \pi + \phi$  (equivalent to a reversal of the nuclear polarization vector  $\vec{J}$ ), we see that  $(\eta + \xi)$  may be determined by measuring the "time-reversal" asymmetry

$$\begin{aligned} A &= [W(\theta_m, \phi_m) - W(\pi - \theta_m, \pi + \phi_m)] / [W(\theta_m, \phi_m) + W(\pi - \theta_m, \pi + \phi_m)] \\ &= [W(\vec{J}) - W(-\vec{J})] / [W(\vec{J}) + W(-\vec{J})] = W_3(\theta_m, \phi_m) / W_1(\theta_m, \phi_m). \end{aligned} \quad (8)$$

### B. Level scheme of $^{131}\text{Xe}$

To obtain a direct measurement of the time-reversal phase  $\eta$ , a transition with negligible final state contribution  $\xi$  is required. In general this condition is satisfied for low  $Z$  nuclei ( $Z < 30$ ) and/or higher energy transitions ( $E > 200$  keV). However, the requirement of an easily polarizable initial nuclear state—hence a large magnetic moment and hyperfine field ( $\Delta/T = \mu B / kT$  on the order of unity)—to some extent restricts the selection of low  $Z$  isotopes. Simultaneously, shielding problems and lower polarization efficiency at high energy place an upper limit on transition energy. The requirements of large mixing ( $\delta \approx 1$ ) and favorable spin coefficients must also be satisfied, as explicitly illustrated by Eq. (7). As a compromise among the various requirements, the prominent 364 keV  $E2$ - $M1$  transition of  $^{131}\text{Xe}$  was selected for measurement of the phase  $\eta$ .

As shown in Fig. 1, the 364 keV level is directly populated from the  $\beta^-$  decay of  $^{131}\text{I}$  (half-life = 8 d). The oriented state is the parent  $^{131}\text{I}$ , which has a magnetic moment  $\mu = 2.738 \pm 0.001 \mu_N$  (Ref. 7). A hyperfine field  $B = 1144.0 \pm 1.5$  kG (Ref. 8) for Fe(I) yields  $\Delta = 32.7$  mK. A large mixing ratio,  $\delta = -4.53 \pm 0.12$ , is reported<sup>9</sup> for the 364 keV transition. Final state calculations<sup>4</sup> give a small final state phase  $\xi = -1 \times 10^{-4}$ .

## III. EXPERIMENTAL METHODS

### A. Source preparation

The Fe( $^{131}\text{I}$ ) sources were prepared by implanting  $^{131}\text{I}^+$  ions into 0.02 mm thick, 0.32 cm diameter iron foils (held at room temperature). Prior to implantation the foils were polished, annealed in  $\text{H}_2$  at 700°C, and indium-soldered to a copper collar button [Fig. 3(a)]. Implantation was performed at Argonne National Laboratory, with acceleration energies of 50 and 70 kV. Source activities of 0.5 to 1 mCi were obtained starting with 30 and 50 mCi of carrier-free  $^{131}\text{I}$  purchased commercially as NaI in 0.05  $N$  NaOH solution. With a mean implantation depth of 0.02  $\mu$ , the  $^{131}\text{I}$  concentration in iron was lower than 0.2 atomic percent.

Upon receipt at the Caltech laboratory, the Fe( $^{131}\text{I}$ ) implanted foil, with activity of about 300  $\mu\text{Ci}$ , was cleaned with alcohol and freon to remove loose surface activity. The collar-button assembly

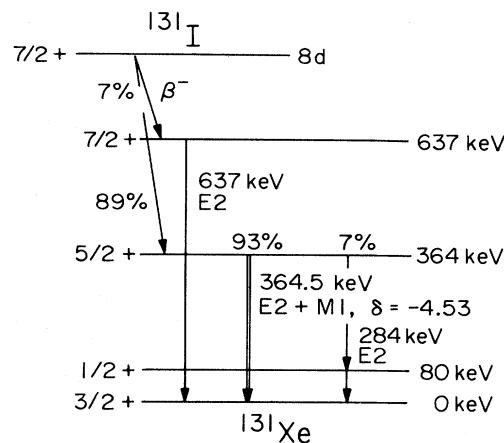


FIG. 1. Decay scheme of  $^{131}\text{I}$ .

was then screwed into the cooling rod of the dilution refrigerator and cooled to 30 mK.

### B. Experimental apparatus

The experimental arrangement is shown in Fig. 2, and described in detail in Ref. 2. Two pairs of orthogonal Helmholtz coils provide a rotatable 2 kG field which saturates the iron foil. The  $^{131}\text{Xe}$  nuclei are polarized via the magnetic hyperfine interaction experienced by the parent  $^{131}\text{I}$  in Fe. A Compton polarimeter, consisting of four NaI(Tl) counters which view source radiation scattered 90° by an Al scatterer, was used to measure the linear polarization of the 364 keV  $\gamma$  ray.

### C. Determination of source temperature and nuclear orientation

The degree of nuclear orientation was determined by measuring with a germanium detector the anisotropy of the 364 keV  $\gamma$  ray emission in the plane of the source. This anisotropy is sensitive to the even orientation coefficients  $B_2(\Delta/T)$  and  $B_4(\Delta/T)$ , whereas the  $T$ -odd term  $W_3$  is proportional to  $B_3(\Delta/T)$ . The extrapolation from  $B_2$  to  $B_3$  is straightforward if all nuclei experience the identical hyperfine field  $B$  (with  $\Delta = \mu B / k$ ). However, anisotropy measurements indicated an effective nuclear orientation systematically lower than expected for a given estimated source temperature. This phenomenon is not unusual for ion-implanted

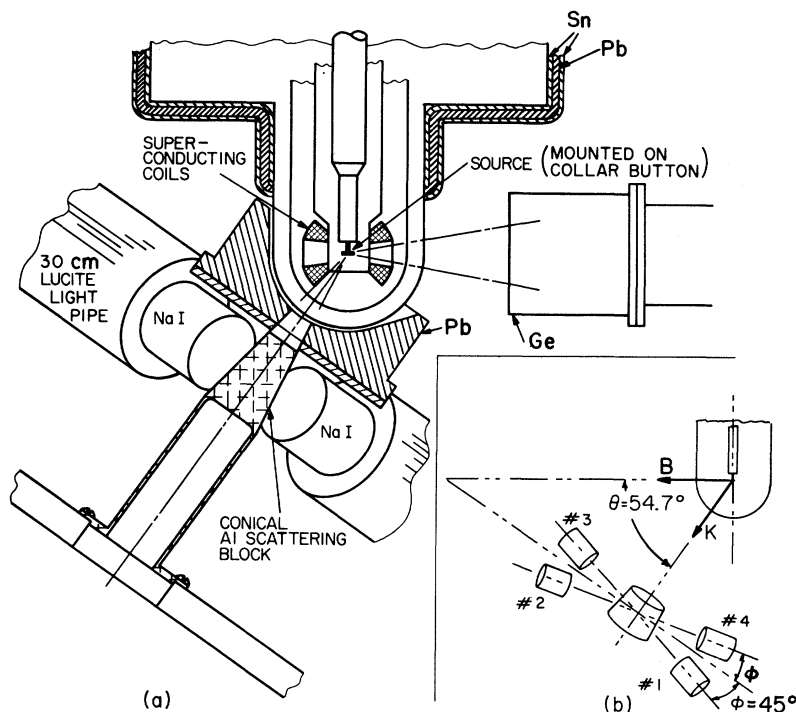


FIG. 2. Schematic representation of the Compton polarimeter. Only two of the four NaI detectors of the polarimeter are shown in the main diagram.

sources,<sup>10</sup> and has been successfully explained in terms of low-hyperfine field siting of some fraction of the  $^{131}\text{I}$  in Fe.<sup>9,11</sup>

To determine an effective third-order coefficient  $B_3$ , a procedure similar to that described in Ref. 2 was adopted. Following the time-reversal experiment, a separate measurement was made to calibrate the 364 keV gamma intensity anisotropy with source temperature determined using an  $\text{Fe}^{60}\text{Co}$  source. This  $\text{Fe}^{60}\text{Co}$  source was prepared as in Ref. 1 by diffusing  $^{60}\text{Co}$  into a 0.02 mm thick iron foil. The foil was indium soldered to a 0.32 cm slotted, threaded copper stud which was tightened down onto the collar-button assembly with a copper nut [see Fig. 3(b)]. [This method circumvented having to solder the  $\text{Fe}^{60}\text{Co}$  to the  $\text{Fe}^{131}\text{I}$  source or to heat the  $\text{Fe}^{131}\text{I}$  foil, and thereby removed the risk of altering the source characteristics we wished to measure. The temperature differential between the two sources was judged to be insignificant.] A two-parameter fit of the observed  $^{131}\text{I}$  anisotropy  $W'(\theta=0^\circ)/W'(\theta=90^\circ)$  to the  $^{60}\text{Co}$ -determined temperature, with

$$W'(\theta) = 1 + \sum_{\lambda=2,4} Q_\lambda f_a B_\lambda(f_s \Delta/T) U_\lambda A_\lambda P_\lambda(\cos\theta), \quad (9)$$

yielded the empirical parameters  $f_a$  (the fraction of  $^{131}\text{I}$  nuclei in high hyperfine field sites) and  $f_s$  (a saturation parameter describing an overall reduction in the average hyperfine field). Values of  $f_a = 0.49 \pm 0.02$  and  $f_s = 0.90 \pm 0.03$  were obtained. This latter parameter corresponds to an effective hyperfine field of 1030 kG, somewhat lower than

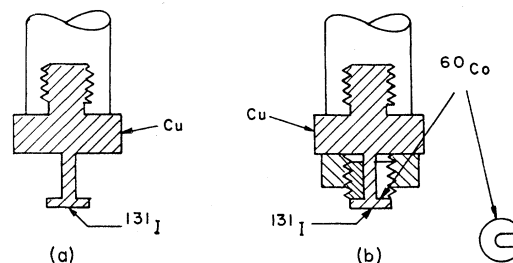


FIG. 3. Source collar buttons.

the NMR-determined field of 1144 kG. Mössbauer studies of Fe(I) indicate the existence of intermediate-field sites,<sup>11,12</sup> so the effective measured field may correspond to a combination of both high and intermediate-field sites.

The Fe( $^{131}\text{I}$ ) sources used in two initial experiments were calibrated by estimating source temperature (to within a few mK) from a temperature-calibrated carbon resistor fixed to the mixing chamber of the refrigerator. For these sources the parameter  $f_s$  was held fixed at  $f_s=0.90$ . Fitting for  $f_a$  yielded  $f_a=0.23\pm 0.01$  and  $f_a=0.48\pm 0.01$ , respectively, for the first and second sources. The much lower alignment obtained for the first source was attributed to an inadequate implantation energy of 50 keV, for which a large proportion of the  $^{131}\text{I}$  resided in the surface oxide layer of the iron foil. An implantation energy of 70 keV yielded the consistent larger values of  $f_a\approx 0.5$ .

The orientation coefficients  $B_{2,4}(\Delta/T)$  were replaced by  $f_a B_{2,4}(f_s\Delta/T)$  for each experiment, and an effective third order coefficient  $B_3(\text{eff})=f_a B_3(f_s\Delta/T)$  was computed.

#### D. Determination of polarimeter efficiency

##### 1. The Compton polarimeter

The Compton polarimeter is shown in Fig. 2. A typical spectrum for a NaI counter is illustrated in Fig. 4. Counts in the single channel analyzer (SCA) energy window of 50 to 300 keV include the (unresolved)  $90^\circ$ -scattered 364 and 284 keV peaks and background from the Compton edges of 364 and 637 keV radiation from the source seen directly by the counters through the shielding.

##### 2. Determination of $E_p$ by Monte Carlo calculation

Because of the high background (background-to-signal ratio  $f=1.5\pm 0.3$ ) and incomplete nuclear orientation of Fe( $^{131}\text{I}$ ), an accurate measurement of the polarimeter efficiency at 364 keV was not feasible. A Monte Carlo program was therefore developed to accurately model the physical geometry of the polarimeter. The calculation yielded a polarization efficiency  $E_p=-0.41\pm 0.03$ , which will be adopted for subsequent discussions. The error reflects the uncertainty in the calculation's reproduction of true polarimeter-source geometry. (The calculation yielded for 122 keV a value  $E_p=-0.45\pm 0.03$ , which is to be com-

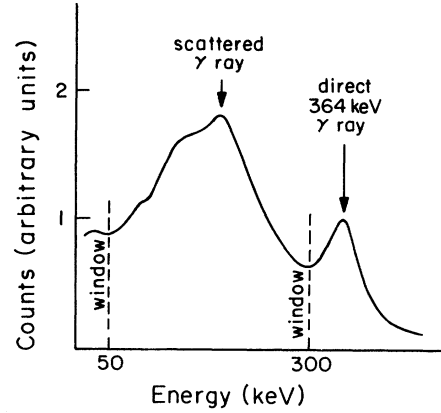


FIG. 4. NaI spectrum of the Compton-scattered 364 keV line of  $^{131}\text{Xe}$ . SCA windows are indicated.

pared with an experimentally measured efficiency<sup>2</sup> for that energy of  $E_p=-0.47\pm 0.01$ .)

##### 3. Experimental corroboration of the Monte Carlo determination

A measurement of  $E_p$  was attempted despite the above-mentioned difficulties. The polarization efficiency is determined by measuring the asymmetry in the  $T$ -even polarization distribution of the transition:

$$A'_p(\theta) = \frac{W'(\theta, \phi=0^\circ) - W'(\theta, \phi=90^\circ)}{W'(\theta, \phi=0^\circ) + W'(\theta, \phi=90^\circ)} \simeq \frac{W_2}{W_1}. \quad (10)$$

The rates  $W'(\theta, \phi)$  represent the total counts in the energy window of Fig. 4. At  $\theta=54.7^\circ$  and  $\theta=90^\circ$ ; adopting an intensity ratio of 93:7 for the 364 and 284 keV lines,<sup>13</sup> we have

$$A_p(54.7^\circ) = E_p \frac{-0.275Q_2f_aB_2 - 0.188Q_4f_aB_4}{1 - 0.132Q_4f_aB_4}, \quad (11)$$

$$A_p(90^\circ) = E_p \frac{-0.412Q_2f_aB_2 + 0.212Q_4f_aB_4}{1 - 0.079Q_2f_aB_2 + 0.127Q_4f_aB_4}. \quad (12)$$

Effective orientation coefficients  $f_a B_\lambda$  are incorporated. Solid angle corrections for the polarimeter are  $Q_2=0.982$ ,  $Q_3=0.963$ , and  $Q_4=0.940$ .<sup>2</sup> The asymmetry  $A_p$  is related to the measured asymmetry  $A'_p$  by<sup>2</sup>

$$A_p = A'_p(1+f) - A_B f,$$

where  $f$  is the background-to-signal ratio and  $A_B$  is the background asymmetry.  $A_B$  was approximated by measuring the asymmetry of Eq. (10) with the Al scatterer of the polarimeter removed. (Alternatively one could obtain a corrected asymmetry  $A_p$  by subtracting a background  $W_{iB}$  from each detector count. The two procedures are essentially equivalent.)

Measured values  $A'_p = 0.0310$  and  $A_B = 0.0024$  were obtained at 25 mK for  $\theta = 90^\circ$ , from which  $A_p = 0.074$  was determined. With  $f_a B_2 = 0.51$  and  $f_a B_4 = 0.12$ , Eq. (12) yields  $E_p = -0.40$ . Similarly, measurements at  $\theta = 54.7^\circ$  gave  $A'_p = 0.0197$  and  $A_B = -0.0084$ , from which a background corrected asymmetry  $A_p = 0.062$  was deduced, yielding  $E_p = -0.39$ . Both measurements are consistent with the adopted value  $E_p = -0.41 \pm 0.03$ .

#### E. Time-reversal asymmetry measurement

The experimental setup for the time-reversal asymmetry measurement is shown in Fig. 2. The asymmetry

$$A' = \sum_{i=1}^4 (-)^{i+1} \frac{W'_i(\vec{B}) - W'_i(-\vec{B})}{W'_i(\vec{B}) + W'_i(-\vec{B})} \quad (13)$$

was computed by comparing count rates for applied fields of opposite polarity ( $\vec{B}$  and  $-\vec{B}$ ), averaging over the four polarimeter counters, and taking into account the fact that counters 2 and 4 (referring to Fig. 2) view opposite polarization patterns relative to counters 1 and 3. The  $W'$  refers to the total integrated count rate within the SCA window depicted in Fig. 4, corrected for source decay. (Typical count rates are on the order of  $1500 \text{ sec}^{-1}$  per counter.) Counting periods between field switching were of 10 min duration. In practice each 10 min run was compared to the average of the previous and following run of opposite field polarity to eliminate to first order the influence of possible temperature or count rate fluctuations (although in reality no such fluctuations were observed).

The background in the spectrum of Fig. 2 dilutes the measured asymmetry. The corrected asymmetry  $A$  of Eq. (8) is obtained from

$$A = A'(1+f). \quad (14)$$

The polarimeter may be positioned at any of four orientations corresponding to the directions (designated N, S, E, and W) defined by the orthogonal pairs of field-generating Helmholtz coils of the dilution refrigerator. Time-reversal data were acquired in pairs of 24 h runs at opposite polarimeter configurations (N and S, and E and W) to average out small geometric or nonsymmetric field-reversal effects.

## IV. RESULTS

Three independent measurements with three  $^{131}\text{I}$  sources have been completed. The experimental parameters, the observed asymmetries, and the resulting phase angles are summarized in Table I. A polarization efficiency  $E_p = -0.41 \pm 0.03$  and a background-to-signal coefficient  $f = 1.5 \pm 0.3$  have been adopted for all three experiments. The higher implantation energy used for the second and third sources is reflected in the improved nuclear polarization. Increased source activity for these latter two experiments resulted in greater statistical precision with a small sacrifice in the minimum attainable source temperature. Asymmetries for the 12 runs of the third experiment, each of approximately 24 h duration, are plotted in Fig. 5.

Included in Table I are the results of control experiments performed at 4 K. No systematic asymmetry was observed for these "warm" runs. Numerous runs have been performed at 4 K for various sources using the present experimental apparatus. Polarimeter count rates have always been consistent with a null asymmetry. We therefore conclude that no systematic asymmetry exists at 4 K and no subtraction of warm runs from cold was performed.

The last column in Table I gives the phase shifts ( $\eta + \xi$ ), determined from the corrected asymmetry  $A$  via Eqs. (7) and (8):

$$\sin(\eta + \xi) = A \frac{1 + Q_4 f_a B_4 U_4 A_4 P_4 (\cos \theta_m)}{R Q_3 f_a B_3 P_3^2 (\cos \theta_m) E_p [|\delta| e^{i\pi} / (1 + |\delta|^2)]} \quad (15)$$

$$= A \frac{1 - 0.123 f_a B_4}{(0.151 \pm 0.004) f_a B_3 E_p}. \quad (16)$$

TABLE I. Summary of  $^{131}\text{Xe}$  experiments. Polarization efficiency  $E_p = -0.41 \pm 0.03$ . Background-to-signal  $f = 1.5 \pm 0.3$ .

Experiment No.	Temperature $T(\text{K})$	Polarization		Raw asymmetry $A' (10^{-5})$	Corrected asymmetry $A (10^{-5})$	Phase $(\eta + \xi) (10^{-3})$
		$f_a \langle B_3 \rangle$	$f_a \langle B_4 \rangle$			
(1)	0.022	-0.15(2)	0.06	2.2(1.9)	5.4(4.8)	5.8(5.3)
(control)	4.0	0.0	0.0	1.2(2.6)		
(2)	0.028	-0.24(3)	0.09	-1.0(1.0)	-2.6(2.5)	-1.5(1.7)
(control)	4.0			0.3(1.4)		
(3)	0.030	-0.22(3)	0.08	-0.9(0.8)	-2.3(2.1)	-1.5(1.5)
(control)	4.0			-0.7(1.0)		
Weighted Average						-1.2(1.1)

In Eq. (16), a 93:7 intensity ratio for the 364 and 284 keV lines was adopted, and numerical values  $|\delta| e^{i\pi} = -4.53 \pm 0.12$  and  $R = -0.1387$  substituted for mixing ratio and spin coefficient. A weighted average of the three experimental values yields  $(\eta + \xi) = (-1.2 \pm 1.1) \times 10^{-3}$ .

## V. DISCUSSION

A phase angle  $(\eta + \xi) \approx \sin(\eta + \xi) = (-1.2 \pm 1.1) \times 10^{-3}$  was measured for the  $(E2, M1)$  transition of 364 keV in  $^{131}\text{Xe}$ . By subtracting the small calculated<sup>4</sup> final state phase for this transition of  $\xi = -0.1 \times 10^{-3}$ , a value of  $\sin\eta = (-1.1 \pm 1.1) \times 10^{-3}$  is obtained. The precision of this measurement is comparable to the best limits in literature [ $\sin\eta < 10^{-3}$  (Ref. 2),  $\sin\eta = (0.3 \pm 0.7) \times 10^{-3}$  (Ref. 1),  $\sin\eta = (1.0 \pm 1.7) \times 10^{-3}$  (Ref. 14),  $\sin\eta = (1.5 \pm 2.2) \times 10^{-3}$  (Ref. 15)], and is consistent with time-reversal invariance.

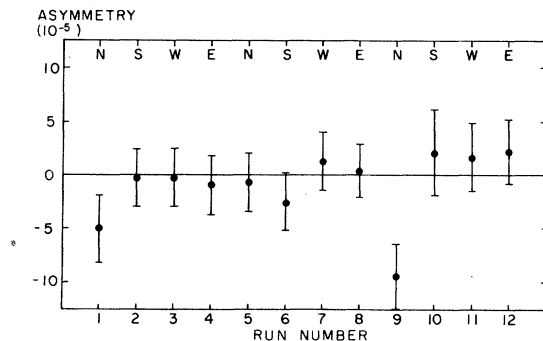


FIG. 5. Asymmetries for the third  $^{131}\text{Xe}$  experiment. Each of the 12 runs is of approximately 24 h duration.

High priority for this experiment was placed on selecting a case where final state corrections were small. A second motivation stems from the present situation that the sensitivity of a given experiment to a time-reversal-violating interaction depends on unknown matrix elements. The possible enhancement of  $T$ -violating matrix elements could increase this sensitivity by orders of magnitude.<sup>16</sup> Theoretical estimates are therefore required to fully realize the implications of a particular experiment. In the meantime it is desirable to measure more than one case with the greatest possible precision.

High precision was obtained with  $^{131}\text{Xe}$  as well as the prior  $^{191}\text{Ir}$  and  $^{57}\text{Fe}$  measurements primarily because they are single counting experiments, in contrast with older coincidence measurements. However, one must measure the relatively insensitive  $\lambda=3$  term rather than the  $\lambda=1$  term in the gamma angular distribution. To achieve high precision requires a nearly ideal combination of large multipole mixing, favorable spin coefficients, and an easily polarizable nucleus. In addition the inherently poor energy resolution of the Compton polarimeter limits the technique to cases where the  $\gamma$ -ray spectrum is simple. A transition with a small atomic final state interaction is also necessary. For the case of  $^{131}\text{Xe}$ , a factor of 2 in increased nuclear polarization could be achieved if temperatures of 10 to 15 mK could be reached. (Present generation dilution refrigerators are able to achieve 10 mK with fairly large source heat loads.) It is doubtful, however, that a sensitivity for  $\sin\eta$  approaching  $10^{-4}$  for time-reversal tests in nuclei could be achieved with any currently available experimental techniques.

## ACKNOWLEDGMENTS

We wish to acknowledge the assistance of N. H. Kwong and E. Redden with the experiment.

Thanks are due to P. Herczeg and P. Vogel for many helpful discussions. This work was supported by the U. S. Department of Energy under Contract No. DE-AT03-81-ER40002.

- 
- <sup>1</sup>N. K. Cheung, H. E. Henrikson, and F. Boehm, Phys. Rev. C 16, 2381 (1977).  
<sup>2</sup>J. L. Gimlett, H. E. Henrikson, N. K. Cheung, and F. Boehm, Phys. Rev. C 24, 620 (1981).  
<sup>3</sup>H. C. Goldwire Jr., and J. P. Hannon, Phys. Rev. B 16, 1875 (1977).  
<sup>4</sup>B. R. Davis, S. E. Koonin, and P. Vogel, Phys. Rev. C 22, 1233 (1980).  
<sup>5</sup>K. S. Krane, Los Alamos Scientific Laboratory Report LA-4677, 1971 (unpublished).  
<sup>6</sup>K. S. Krane, Nucl. Data Tables 11, 407 (1973).  
<sup>7</sup>E. Lipworth, H. L. Garvin, and T. M. Green, Phys. Rev. 119, 2022 (1960).  
<sup>8</sup>P. K. James, N. J. Stone, and H. R. Foster, Phys. Lett. 48A, 237 (1974).  
<sup>9</sup>B. K. S. Koene and H. Postma, Nucl. Phys. A219, 563 (1974).  
<sup>10</sup>P. G. E. Reid, M. Sott, N. J. Stone, D. Spanjaard, and H. Bernas, Phys. Lett. 25A, 396 (1967).  
<sup>11</sup>H. deWaard, R. J. Cohen, S. R. Reintsema, and S. A. Drentje, Phys. Rev. B 10, 3760 (1974).  
<sup>12</sup>V. Visser, L. Niesen, H. Postma, and H. deWaard, Phys. Rev. Lett. 41, 882 (1978).  
<sup>13</sup>R. L. Auble, H. R. Hiddleston, C. P. Browne, Nucl. Data Sheets 17, 573 (1976).  
<sup>14</sup>O. C. Kistner, Phys. Rev. Lett. 19, 872 (1967).  
<sup>15</sup>G. W. Wang, A. J. Becker, L. M. Chirousky, J. L. Groves, and C. S. Wu, Phys. Rev. C 18, 476 (1978).  
<sup>16</sup>W. A. Steyert and K. S. Krane, Phys. Lett. 47B, 294 (1973).